High Energy Density Physics 9 (2013) 204–208

Contents lists available at SciVerse ScienceDirect

High Energy Density Physics

journal homepage: www.elsevier.com/locate/hedp

Short communication

Nearest-neighbor atom interference effect on bound-free opacity of hot dense gold plasma

Yong Hou [a], Jianhua Wu [a], Jianmin Yuan [a,b,*]

[a] Department of Physics, National University of Defense Technology, Changsha 410073, PR China
[b] State Key Laboratory of High Performance Computing, National University of Defense Technology, Changsha 410073, PR China

ARTICLE INFO

Article history:
Received 29 September 2012
Received in revised form
25 December 2012
Accepted 27 December 2012
Available online 4 January 2013

Keywords:
Hot dense plasma
Quantum interference
Opacity

ABSTRACT

Quantum interference, similar to Young double-slit interference, takes place between the photoionization processes of two same kind atoms when the nuclei separation is less than or comparable to the de Broglie wavelength of the ionized electrons. In dense plasma, the average nearest-neighbor atom distance maybe comparable to or even less than the wavelength of the outgoing electrons, the photoionization cross section of the atoms as well as the opacity of the plasma will be affected by this kind of interferences among atoms. In the present work, we first attain the nearest-neighbor distributions of the atoms in hot dense plasmas by performing an average-atom molecular dynamics (AAMD) simulation. Then, the effective total photoionization cross section is obtained by integrating the two atom interference effects over the nearest-neighbor distributions. At last, the bound-free and Rosseland mean opacities of Au plasmas at 100 eV and different densities show that the interference effects are considerable when the density is larger than 1 g/cm^3.

Opacity is a fundamental quantity used in astrophysics [1], inertial confinement fusion (ICF) [2] and X-ray lasers. Many experimental and theoretical studies on opacity have been performed at high temperatures and low densities [3–8]. With the development of laser techniques, more and more dense plasmas have been produced in the experiment [9]. So we should consider the effect of dense environment in calculating the opacities of hot dense plasmas. We have studied the opacity of solid-dense Al plasmas considering the dense environment in calculating the atomic data [10]. In the present work, we will study the interference effect between photoionization processes of neighboring atoms on the opacity of hot solid-dense Au plasma.

In the photoionization processes, quantum interference between atoms may happen when the separation between the atoms is comparable to or less than the wavelength of the concerned electron. One of this kind interference was first suggested theoretically by Cohen and Fano in 1966 [11], who considered that electron emission from the inner core orbitals of diatomic molecules in the photon-energy regime of a few hundreds eV would interfere. Until 2001, Stolterfoht et al. [12] observed interference patterns in the experimental electron ionization spectra of H_2 interacting with 60 MeV/u-Kr34 projectiles. After that, significant interest has been focused on studying interference phenomena involving homonuclear molecules [13–27]. In the references, they all considered that the photoionizations of the homonuclear diatomic molecule can be regarded as a molecular Youngs double-slit experiment where the emission of the spherical electron waves originating from two spatially separated sources gives the interference patterns. And the photoionization cross sections will be modulated by the nearest-neighbor atoms [28] when the de Broglie wavelength of the ionized electron is larger than or comparable with the two atoms distance. In fact, in dense plasmas when the distance of nearest-neighbor ions is so small that can be comparable with the wavelength of photoionized bound electrons, the emission electrons from the nearest-neighbor ions will be influenced. So the interferences effect on the bound–free (B–F) opacity should be considered in hot dense plasma regions.

In the present work, we first perform the average-atom molecular dynamics (AAMD) [29] using the pair-potential, which includes the thermal electron excitation and ionization in a statistical way, to obtain the nearest-neighbor ionic distributions. And then, we consider the nearest-neighbor ions interferences effects on the total photoionization cross sections according to the Cohen and Fano's pattern. Finally, the B–F and Rosseland mean opacities of gold are given and compared with the results without the nearest-neighbor ionic interference.

* Corresponding author. Department of Physics, National University of Defense Technology, Changsha 410073, PR China.
E-mail addresses: yonghou@nudt.edu.cn (Y. Hou), jmyuan@nudt.edu.cn (J. Yuan).

1574-1818/$ – see front matter © 2013 Elsevier B.V. All rights reserved.
http://dx.doi.org/10.1016/j.hedp.2012.12.011

The electronic structures are calculated in a full relativistic self-consistent field average-atom (AA) model which is one of the statistical approximations applied to calculations of electronic structure of atoms and ions in hot and dense plasmas based on the statistical average over the details of the populations of ions and occupations of the electronic energy levels [30–34]. The movement of an electron is approximated by a central-field, which is formed by the nucleus and other electrons. However, in dense environment, the spherically symmetric potential will be broken by the interactions between ions, and the electronic distributions will be affected. To include the effects in the AA model, we have treated the bound energy levels as the energy bands with a Gaussian distributions of density of state, which is normalized to ensure that the integration of the density of state over one band is equal to the statistical weight of the corresponding atomic level. The results affect greatly the mean ionization degree and equation of state [35]. The free electrons are considered more simply with an assumption of the temperature dependent Thomas–Fermi (TF) [36] treatment.

Contributions to the total opacity consist of four parts

$$K_\nu = \frac{N_A}{A} \times \left[\sigma^{bb}(h\nu) + \sigma^{bf}(h\nu) + \sigma^{ff}(h\nu)\right] \times \left[1 - \exp\left(-\frac{h\nu}{k_B T}\right)\right] + K_{sc} \tag{1}$$

where N_A is Avogadro constant, A is the atomic weight, and k_B is the Boltzmann constant. The contributions of the bound–bound (B–B) and B–F transitions, σ^{bb} and σ^{bf}, take only the electric dipole term. The free–free contributions, σ^{ff}, are calculated from the Kramer's cross section, and the scattering contribution, K_{sc}, is obtained using the Thomson scattering cross section.

In dense plasmas, the quantum interference effects may occur during the single photoionization process when the ion–ion distance is compared with the wavelength of the ionized electrons, which will affect the B–F cross sections. To investigate the interference effects, we apply a formalism analogous to that developed for electron elastic scattering from two atoms [37], which have been discussed by Stolterfoht et al. [12]. The photoionization cross section from two atoms or ions can be written as

$$\frac{d\sigma_{N-N}}{d\Omega d\varepsilon d\mathbf{k}} = \frac{d\sigma_{2N}}{d\Omega d\varepsilon d\mathbf{k}}[1 + \cos(\mathbf{k}\cdot\mathbf{d})] \tag{2}$$

where the cross section $d\sigma_{N-N}/d\Omega d\varepsilon d\mathbf{k}$ describes the photoionization cross section from the two atoms or ions separated by $\mathbf{d}$ while the cross section $d\sigma_{2N}/d\Omega d\varepsilon d\mathbf{k}$ refers to that of two atoms or ions acting at independent particles. The solid angle $d\Omega$ and the energy $d\varepsilon$ refer to the outgoing electron. The vector $\mathbf{k}$ is the momentum of the ionized electron, while $\mathbf{d}$ is the vector associated with the internuclear distance of the two atoms or ions. After performing an average over the orientations of the internuclear axis of the two neighboring atoms or ions, we obtain the relationship

$$\frac{d\sigma_{N-N}}{d\Omega d\varepsilon dk} = \frac{d\sigma_{2N}}{d\Omega d\varepsilon d\mathbf{k}}\left[1 + \frac{\sin(kd)}{kd}\right] \tag{3}$$

The term in the parenthesis represents the interference caused by the two neighboring atoms or ions.

In hot dense plasmas, the distance of the nearest-neighbor ion will change due to the ions moving. Therefore, the quantum interference effects on the photoionization cross sections will change with time. In order to consider the effects, we integrate the nearest-neighbor distributions when we calculate the effective

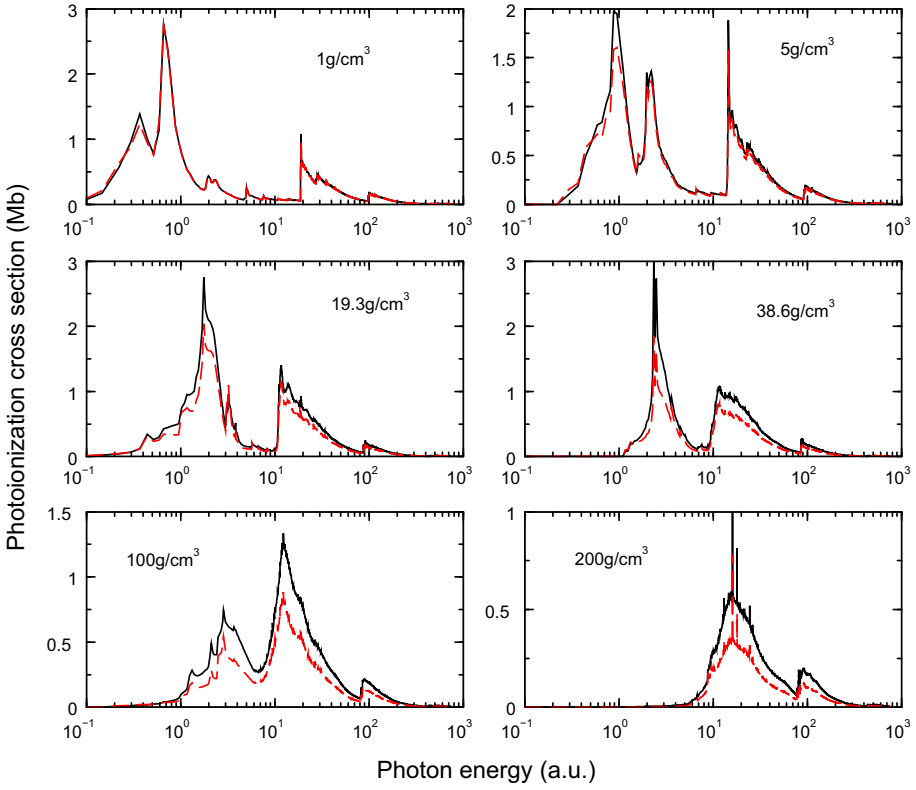

Fig. 1. The total photoionization cross sections of Au with (red dashed lines) and without (black solid lines) the quantum interference of the nearest-neighbor ions at the temperature 100 eV and different densities, respectively. (For interpretation of the references to color in this figure legend, the reader is referred to the web version of this article.)

photoionization cross sections. The nearest-neighbor distributions are obtained from the AAMD [29].

When the plasmas and radiation are in thermodynamic equilibrium, the Rosseland mean opacity is often used to describe radiation transport in optically thick materials, which are defined by

$$\frac{1}{K_R} = \int \frac{W_R(u)\mathrm{d}u}{K_\nu} \tag{4}$$

where $u = h\nu/k_BT$, and W_R are Rosseland weighting functions,

$$W_R(u) = \frac{15}{4\pi^4}\frac{u^4 e^{-u}}{(1-e^{-u})^2} \tag{5}$$

We first calculate the nearest-neighbor distributions using the AAMD [29]. In hot dense plasma, the electronic structures are obtained from the AA model [35], which has considered the energy broadening due to the ion–ion strong interaction. And in the frame of temperature-depended density functional theory (TDDFT), we calculate the ion–ion pair potentials through modifying the Gordon and Kim (GK) [38,39] theory. Classical molecular dynamics are performed to get the statistical properties of ionic structures. And then, we consider the quantum interference of the photoionization cross sections through integrating all the possible nearest-neighbor ionic distance.

In Fig. 1, we give the total photoionization cross sections of Au at the temperature 100 eV and different densities (1 g/cm^3, 5 g/cm^3, 19.3 g/cm^3, 38.6 g/cm^3, 100 g/cm^3, 200 g/cm^3). Solid (black) lines and long dashed (red in the web version) lines represent the results without and with the interference effects, respectively. At the density 1 g/cm^3, the two lines are almost the same except for the energies near the threshold. However, with the density increasing, the difference becomes more considerable. In particular, at the density 100 g/cm^3, 4*d* photoionization cross section without the interference is almost twice than that with the interference at the tip near the photon energy of 10 a.u. However, for all densities in the figures, the two lines go close to each other when the photon energy is far away from the threshold. The phenomena are similar to the Youngs double-slit interference experiment. At low density, the distance of the nearest-neighbor ions is very large, which is alike as the distance of the double-slit, even though the wavelengths of the outgoing electrons are very long, the phenomena of the interference are not obvious. So at the density 1 g/cm^3, the interference can be observed only just above the threshold. The distance of the nearest-neighbor ions becomes smaller with the density increasing, we can observe the interference of outgoing electrons in the wider energy region. When the energy of the photoelectron is so large that the ionized electron wavelength is far smaller than the distance of the nearest-neighbor ions, the phenomena of interference will disappear. So in the figures two kinds of lines will come closer at the energy of outgoing electron far from the threshold. In addition, we find the results with interference effects are larger than that without interference effects in low photon energies, such as the figure of 5 g/cm^3. In fact, the bound electrons near the energy limit have such low energy that the wavelengths are very large, the interference effects are very considerable, therefore, the photoionization cross sections with the interference of the low energy electrons are larger than that without the interference just above the threshold, see Fig. 2. In Fig. 2, we give the photoionization cross sections of 4*s*,4*p*, and 4*d* at the density 19.3 g/cm^3. We can see that the photoionization cross sections with considering the quantum interference are larger in the low energy region, however, smaller in the high energy region than that without considering the quantum interference. This tells us that the interferences effect not only depend on the distance of ions, but also on the energies of outgoing electrons.

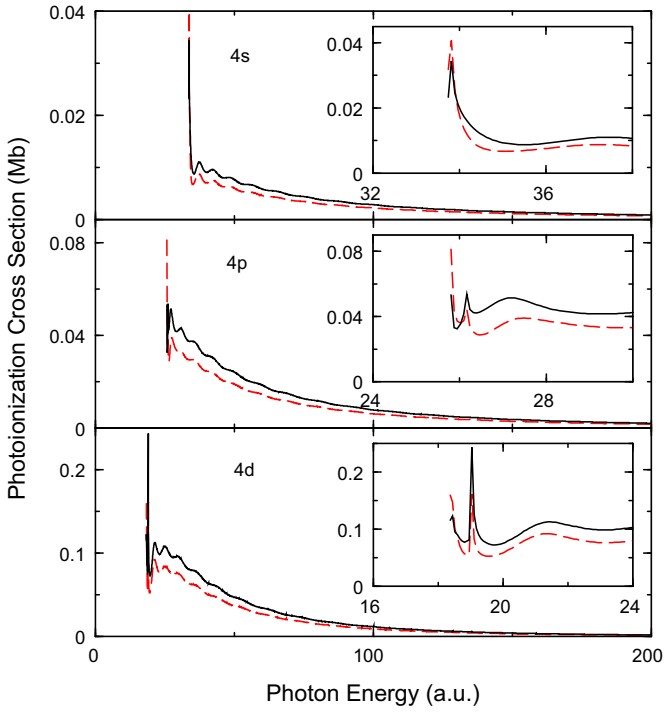

Fig. 2. The comparison of photoionization cross sections of 4*s*, 4*p*, and 4*d* with and without interference effects at temperature 100 eV and density 19.3 g/cm^3. In the insets, photoionization cross section just above the threshold is shown.

In order to consider the interference effects on opacity, we calculated the B–F opacity of Au in hot dense plasma regions. In Fig. 3, we give the B–F opacities at the temperature 100 eV and different densities. It is very similar that the interference effects on the B–F opacity with the photoionization cross section. At low densities, the interference effects on the B–F opacities can be observed only just above the threshold, and with the density increasing, the difference becomes more and more obvious. In addition, the positions of the tips contributed by different bands, will move to the lower energy with the density increasing due to the ionization potential depression (IPD). And the tips first become higher and then become lower with the density increasing due to the pressure ionization. Especially, at the density 200 g/cm^3, the tips contributed by the 5*n* band disappear. So the interference effect contributions to the total Rosseland mean opacities from the B–F opacities first increase and then decrease with the density increasing, see Fig. 4. In the figure, we give the Rosseland mean opacities with interference effects (red long dashed line in the web version) and without interference effects (black solid line). In the inset, the percent of the decrement is given. From these data, one can see that the effect on the Rosseland mean opacities is not linear increase even though the effects on the B–F opacities are more considerable with the density increasing. At higher densities, the electrons of bound states become induced, especially, 5*n* electrons at the density 200 g/cm^3 disappear, due to the pressure ionization. And the B–F contributions to the total opacities will decrease.

In the above discussion, the influence of the lifetimes of quasi-molecular states on the photo ionization processes is not included, since the photoelectron is considered to be nonlocal when we discuss the quantum interference effect. The time compared with the lifetime of the so-called quasi-molecular should be the transition time of the photoionization process. The ionization time,

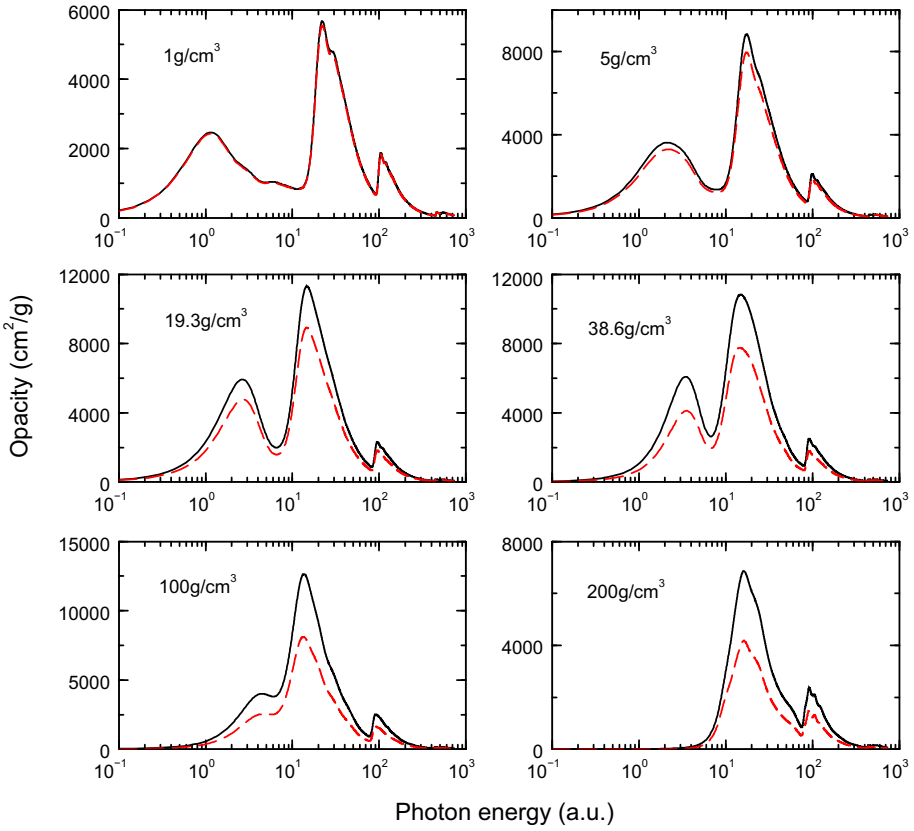

Fig. 3. The bound–free opacities of Au with (long dashed red lines) and without (solid black lines) the quantum interference of the nearest-neighbor ions at the temperature 100 eV and different densities. (For interpretation of the references to color in this figure legend, the reader is referred to the web version of this article.)

according to the uncertainty relation, could be estimated from the transition, which are normally from hundreds to thousands eV for inner shell electrons. The photoionization time of the deep bound electrons is much shorter than the lifetimes of quasi-molecular states, which are determined by the thermal motion of the ions. For example, the Au plasma at the density 19.3 g/cm^3 and temperature 100 eV, the ionic movement of $R/100$ (R is the mean ionic distance) takes the time of 15.2 a.u., while the ionization time of the bounds electron with the ionization energy of 1 a.u. is 6.283 a.u. at most. However, the lifetimes of quasi-molecular states will have an influence on the near threshold photoionization of electrons at the Rydberg states just below the ionization limit. Because when the ionization potential of the bound electron energy is smaller than 0.4 a.u., the ionization time is longer than 15.2 a.u. Under the condition, the ionic movement will affect the ionization process of the electrons populating at the Rydberg states. For the problem discussed in the paper, those states are less populated and the total results, obtained by averaging over the nearest ionic distribution, are hardly affected by the ionic dynamic effects.

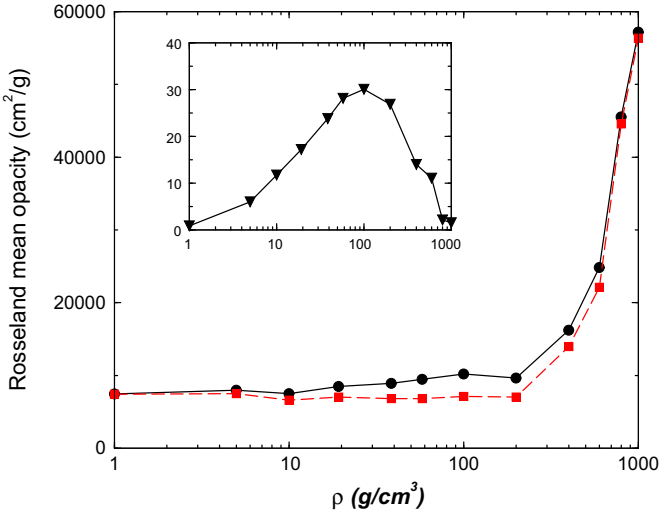

Fig. 4. The Rosseland mean opacities of Au at the temperature 100 eV and different densities. The solid (black) and long dashed (red) lines are the results without and with interference, respectively. In the inset, the percent of the decrement is given. (For interpretation of the references to color in this figure legend, the reader is referred to the web version of this article.)

In the hot dense plasma, the photoelectrons will become localized due to collision with other particles, and the effect of quantum interference is suppressed. So we would estimate the dephasing effects through comparing the mean ionic distance (R) with the mean free paths (MFP) of the photoelectrons. The mean free paths (MFP) of the photoelectrons are calculated by $\lambda(\omega=0)=v_e/\nu(\omega=0)$, where v_e, $\nu(\omega=0)$ are photoelectron velocity and collision frequency, respectively. And $\nu(\omega=0)$ is taken in the Born approximation [40]. The photoelectron velocity is equal to $2\pi/R$ (R, mean ionic distance, a. u.) when the de Broglie length of photoelectron is equal to R. From the Table 1, the mean free paths are much larger than mean ionic distance when the velocity of photoelectron is equal to the $2\pi/R$ (a.u.), so the dephasing effects will almost not affect the quantum interference in the temperature–density regime discussed.

In conclusion, one kind of the nearest-neighbor atom interferences effects, similar to the Young's double-slit interference phenomena, on the opacity in hot dense plasma has been

Table 1
The mean free paths (MFP) and mean ionic distance are given using in atomic unit at the temperature 100 eV and different densities.

ρ g/cm^3	1	5	19.3	38.6	100	200
MFP	78.6	40.9	26.3	21.8	20.5	22.3
R	8.08	4.73	3.01	2.39	1.74	1.38

considered. With the plasma density increasing, the quantum interferences effects on the bound–free (B–F) opacities are more obvious. However, at low density the interferences on photoionization cross sections are obvious only just above the threshold. It is shown that the interferences depend on not only the distance of the nearest-neighbor atom or ion, but also the de Broglie wavelength of the outgoing elections. So the results tell us that the quantum interferences should be considered when we calculate the opacity and use the spectrum to diagnose the temperature and density in hot dense plasma regions.

Acknowledgments

This work was supported by the National Natural Science Foundation of China under Grant Nos. 11005153, 11104350. Funding support (SKLLIM1107) from State Key Laboratory of Laser Interaction with Matter is acknowledged.

References

[1] F.J. Rogers, C.A. Iglesias, Science 263 (1994) 50;
C.A. Iglesias, et al., Astrophys. J. 445 (1995) 855.
[2] E. Storm, J. Fusion Energy 7 (1988) 131;
R.L. Kauffman, et al., Phys. Rev. Lett. 73 (1994) 2320.
[3] M.J. Seaton, J. Phys. B 20 (1987) 6363.
[4] C.A. Iglesias, F.J. Rogers, Astrophys J. 464 (1996) 943;
C.A. Iglesias, et al., J. Quant. Spectrosc. Radiat. Transf. 81 (2003) 227.
[5] P. Hakel, et al., J. Quant. Spectrosc. Radiat. Transf. 99 (2006) 265.
[6] J.L. Zeng, et al., Phys. Rev. E 62 (2000) 7251;
J.L. Zeng, J.M. Yuan, Q.S. Lu, Phys. Rev. E 64 (2001) 066412;
C. Gao, J.L. Zeng, Phys. Rev. E 78 (2008) 046407.
[7] J. Bailey, et al., Phys. Rev. Lett. 99 (2007) 265002.
[8] A. Rickert, J. Quant. Spectrosc. Radiat. Transf. 54 (1995) 325.
[9] O. Ciricosta, et al., Phys. Rev. Lett. 109 (2012) 065002.
[10] Y. Li, et al., J. Phys. B 42 (2009) 235701.
[11] H.D. Cohen, U. Fano, Phys. Rev. 150 (1966) 30.
[12] N. Stolterfoht, et al., Phys. Rev. Lett. 87 (2001) 023201;
N. Stolterfoht, et al., Phys. Rev. A 67 (2003) 030702(R).
[13] F. Lindner, et al., Phys. Rev. Lett. 95 (2005) 040401.
[14] K. Kreidi, et al., Science 318 (2007) 949.
[15] J. Fernandez, et al., Phys. Rev. Lett. 98 (2007) 043005.
[16] B. Zimmermann, et al., Nat. Phys. 4 (2008) 649.
[17] K. Kreidi, et al., Phys. Rev. Lett. 100 (2008) 133005.
[18] C.D. Lin, et al., J. Phys. B 43 (2010) 122001.
[19] N.A. Cherepkov, et al., Phys. Rev. A 82 (2010) 023420.
[20] D.S. Milne-Brownlie, et al., Phys. Rev. Lett. 96 (2006) 233201;
J. Gao, D.H. Madison, J.L. Peacher, Phys. Rev. A 72 (2005) 032721.
[21] D. Misra, et al., Phys. Rev. Lett. 92 (2004) 153201;
S. Chatterjee, et al., J. Phys. B 43 (2010) 125201.
[22] C. Dimopoulou, et al., Phys. Rev. Lett. 93 (2004) 123203.
[23] H.T. Schmidt, et al., Phys. Rev. Lett. 101 (2008) 083201.
[24] L. Ph, H. Schmidt, et al., Phys. Rev. Lett. 101 (2008) 173202.
[25] J.S. Alexander, et al., Phys. Rev. A 78 (2008) 060701(R).
[26] C.A. Tachino, et al., J. Phys. B 43 (2010) 135203. J. Phys. Conf. Ser. 288 (2011) 012026.
[27] A.B. Voitkiv, et al., Phys. Rev. Lett. 106 (2011) 233202.
[28] J. Wu, J. Yuan, Chin. Phys. B 18 (2009) 5283.
[29] Y. Hou, J. Yuan, Phys. Rev. E 79 (2009) 016402.
[30] B.F. Rozsnyai, Phys. Rev. A 5 (1972) 1137. J. Quant. Spectrosc. Radiat. Transf. 27 (1982) 211;
B.F. Rozsnyai, M. Lamoureux, J. Quant. Spectrosc. Radiat. Transf 43 (1990) 381.
[31] G. Faussurieri, C. Blancard, A. Decoster, Phys. Rev. E 56 (1997) 3474. ibid. 56 (1997) 3488.
[32] D.A. Liberman, Phys. Rev. B 20 (1979) 4981. J. Quant. Spectrosc. Radiat. Transf. 27 (1982) 335.
[33] W.R. Johnson, High Energy Density Phys. 5 (2009) 61–67.
[34] J. Yuan, Phys. Rev. E 66 (2002) 047401. Chin. Phys. Lett. 19 (2002) 1459.
[35] Y. Hou, F. Jin, J. Yuan, Phys. Plasmas 13 (2006) 093301. J. Phys. Condens. Matter 19 (2007) 425204.
[36] L.H. Thomas, Proc. Camb. Philos. Soc. 23 (1927) 542;
E. Fermi, Z. Phys. 48 (1928) 73.
[37] A. Messiah, Quantum Mechanics, vol. II, Amsterdam, North-Holland, 1970, pp. 848–852.
[38] R.G. Gordon, Y.S. Kim, J. Chem. Phys. 56 (1972) 3122;
Y.S. Kim, R.G. Gordon, Phys. Rev. B 9 (1974) 3548.
[39] J. Yuan, Y. Zhao, Z. Zhang, Acta Mech. Sin. 21 (1989) 479 (in Chinese).
[40] R. Thiele, R. Redmer, H. Reinholz, G. Ropke, J. Phys. A Math. Gen. 39 (2006) 4365–4368.